







## Research Article

# Tribological Behavior of Ni-P Electroless Coating of Inconel 625 with Multiwall Nano Carbon Tubes

**D. Jayabalakrishnan** <sup>1</sup>, **S. Senthil Kumar** <sup>2</sup>, **R. Suthan** <sup>3</sup>, **P. Babu Aurtherson** <sup>4</sup>,  
**J. Elanchezhian**,<sup>5</sup> **V. Ramanareddy**,<sup>6</sup> **S. Louies Praveen** <sup>7</sup>,  
**and Umamaheswari Kandasamy** <sup>8</sup>

<sup>1</sup>Center for Materials, Chennai Institute of Technology, Chennai 600069, India

<sup>2</sup>Department of Mechanical Engineering, R.M.K College of Engineering and Technology, R.S.M Nagar, Pudukkottai, Thiruvallur 601206, India

<sup>3</sup>Department of Mechanical Engineering Panimalar Engineering College, Chennai 600123, India

<sup>4</sup>Department of Mechanical Engineering, DMI Engineering College, Aralvaimozhi, Kanyakumari, Tamil Nadu, India

<sup>5</sup>Department of Mechanical Engineering, Anand Institute of Higher Technology, Chennai 603103, India

<sup>6</sup>Department of Mechanical Engineering, Vardhaman College of Engineering, Hyderabad 501218, Telangana, India

<sup>7</sup>Department of Mechanical Engineering, Panimalar Institute of Technology, Chennai 600123, India

<sup>8</sup>Kebridehar University, Kebridehar, Ethiopia

Correspondence should be addressed to Umamaheswari Kandasamy; umasashwini@gmail.com

Received 24 June 2022; Revised 26 September 2022; Accepted 14 October 2022; Published 24 July 2023

Academic Editor: R. Thanigaivelan

Copyright © 2023 D. Jayabalakrishnan et al. This is an open access article distributed under the Creative Commons Attribution License, which permits unrestricted use, distribution, and reproduction in any medium, provided the original work is properly cited.

An attempt was taken to study the wear rate of coated Inconel 625 using 0.3 gm of multiwall carbon tubes (MWCNT). The coating was carried out by the Ni-P electroless coating method. The Ni-P-MWCNT coating was prepared by using nickel phosphorous solution. The sliding wear test was conducted using pin on discs tribometer. The wear rate behavior was investigated at various levels of pin on discs tribometer factors, and a predictive model was developed using regression equations. The wear test experiment was carried out based on the  $L_{27}$  orthogonal array. The wear process parameters load, sliding velocity, and sliding distance were chosen. It was observed that the rate of wear increased as the load increases, whereas increase in sliding velocity and sliding distance reduces the rate of wear. The developed regression model was validated with the measured wear rate. The percentage error was observed within 0.99%.

## 1. Introduction

Inconel alloy is used in automotive, aerospace, and defense industries due to its high-strength and corrosion resistance [1, 2]. Inconel 625 alloy is widely utilized in different area owing to its features such as high work hardening rate and low thermal conductivity. This alloy is particularly used to make turbine blades, aero engine parts, and heat exchangers parts. Inconel 625 is subjected to high temperature environment, and its alloy wear and corrosion resistivity need to be improved in order to withstand the impact of high temperature environment. Naji et al. [3] have studied the

corrosion resistivity, biocompatibility of HA/TiO<sub>2</sub>, and ZrO<sub>2</sub>/HA coating material. Titanium alloy (Ti-6Al-7Nb) was used as substrate material. The anodic microarc oxidizing (MAO) coating technique was used. They have reported that the rutile and anatase phases were present by MAO coating. Furthermore, they have said that the metaphosphates were seen by mixing ZrO<sub>2</sub> to the electrolyte. Guo et al. [4] have studied the effect of nano tubes-coated Ti6Al4V alloy on wear and corrosion resistivity and microstructure. They have carried out coating process on this alloy using various concentric level of sodium chloride solution, and the coating was done by microarc oxidation. They have suggested that

0.15 Gram/liter CNT has shown low porosity and roughness. The corrosion resistivity was enhanced on increasing the CNT concentration up to 0.15 Gram/liter.

Li et al. [5] have done using microarc oxidation coating on Zr alloy substrate using composite coat  $\text{Al}_2\text{O}_3/\text{MoS}_2/\text{CeO}_2/\text{graphene oxide}$ . They have investigated the surface status, cross section status, composition, and structure of phase of various composite microarc oxidation coating. They have suggested that the composite coating consisting  $\text{ZrO}_2$  s hashown better corrosion resistance and the MAO coating— $\text{Al}_2\text{O}_3$  has shown the good resistivity of corrosion.

Askarnia et al. [6] have coated the surface of AZ91 magnesium alloys using various amounts of graphene oxide and they have used microarc oxidation process in the presence of alkaline electrolyte. The test of scratch, behavior of corrosion, antibacterial and bioactivity properties of coated AZ91 magnesium alloys were carried out. They have observed that the  $\text{MgO}$  and  $\text{Mg}_2\text{SiO}_4$  ceramics were existed as a result of oxidation and electrolyte reaction. The surface of AZ91 magnesium alloy coated with 20 mg/L of GO leads to minimum pores on the surface. The crashed width of the scratch reduced from about  $137\ \mu\text{m}$  to  $87\ \mu\text{m}$  for sample coated with 20 mg/GO owing to strengthening of the coating by graphene oxide reinforcement. Küçükosman et al. [7] have deposited composite coat on AZ91 alloy using MAO (microarc oxidation) and the MAO-hydrothermal treatment. Si/ph-based electrolyte/graphite particles size of 5–10 and  $75\ \mu\text{m}$  were used. The surface morphology with good appearance was observed in the MAO coating, and also the resistance of wear of the graphite-doped MAO-HT composite coatings was improved identically.

Thanu et al. [8] have used electro deposition of Ni-Ta coating on Nickel-based alloy. Their study revealed that the scanning electron microscopic shows evidently that constant electro deposition generates smooth and uniform coatings. Higher hardness was achieved in the coating done using Ni/Ta: 4 : 1 and it increases to 270 VHN. Reis et al. [9] stated that copper-beryllium is the materials which are widely utilized to make mold in the injection moulding process. Though it has great abrasion resistance, still its resistivity needs to be improved. Therefore, this material is coated using Ni-P coating. They have investigated the hardness, wear test, XRD, and SEM analysis, and the improvement of the coated alloy behavior is reported.

Corona-Gomez et al. [10] stated that radio-frequency magnetron sputtering is used to coat TaZrN on CoCrMo biomedical substrate. The wear and corrosion behaviour in addition to mechanical test of the coated substrate is evaluated. They have reported that the coated specimen has proved lower wear rate and higher corrosion resistivity. Finally, they have said that the coated specimen would improve the hip joint implant's lifetime. Wei et al. [11] reported the wear and corrosion resistivity of coated AZ31 magnesium alloy. The alloy was coated with Al using the magnetron sputtered method after that the coated specimen is treated using plasma electrolytic oxidation (PEO). The aluminate and silicate electrolytes are used for PEO. They

have resulted that the aluminate produces better wear resistivity than silicate coat of the specimen. Furthermore, the PEO/Al has improved the corrosion resistivity of AZ31 alloy.

Ma et al. [12] have studied the corrosion and wear resistance including morphology of Mg-Li-coated alloy by adding Al-Y. The microarc oxidation coatings are used. The best corrosion resistance, wear resistance enhanced hardness, and minimum porosity were obtained for Mg-14Li-3Al-1Y alloy. Jiang et al. [13] have investigated the behaviour of microstructure, microhardness, and wear resistance of WC-Co coating on Ti-6Al-4V substrate. The laser cladded coating method is used to coat Ti-6Al-4V substrate. They have seen an improvement in microhardness and wear resistivity of WC-Co coating on Ti-6Al-4V substrate. Qin et al. [14] have deposited  $\text{SiO}_2\text{-Ni}$  on AZ<sub>91</sub>D substrate using electroplating technique, characterized by AFM, SEM, and mechanical and tribological test. It has found that the corrosion resistivity was more improved owing to composite coating than pure Ni coating. Furthermore, it was noticed that the  $\text{SiO}_2\text{-Ni}$  composite coat has shown great wear resistance. Divya Sadhana et al. investigated the wear characteristic-Specific Wear Rate-is optimized using the Taguchi approach (SWR) [15]. Physical Vapor Deposition (PVD)-based AlTiN can be applied to coat titanium alloy and SS 316LVM materials for biomedical applications since it has greater wear resistance qualities [16, 17]. An innovative multistage micromechanical approach is proposed to explore the function of carbon nanotube (CNT) coating on carbon fibre (CF) surfaces in the effective thermal conductivities of the unidirectional polymer hybrid nanocomposites [18].

The polarisation efficiency of poly (vinylidene fluoride)/barium titanate (PVDF/ $\text{BaTiO}_3$ ) composites was increased by coating carbon nanotubes [19]. Titanium alloy was coated with carbon nanotubes (CNTs)-reinforced composites using a laser cladding. Due to the self-lubricating effect, the coating's COF was drastically lowered [20]. Analysis of wear characteristics of titanium nitride had been deposited by DC magnetron sputtering over 6061 aluminium alloy. The Vickers hardness tester was used to assess the hardness of untreated and coated aluminium specimens, and the findings showed that coated specimens had a 26% improvement in comparison to uncoated samples [21].

From the literature review, it is evidently seen that there was no adequate investigation on coated Inconel alloy. Therefore, an attempt is taken to study the MWCNT-coated Inconel 625 using electroless coating technique. The wear rate was observed and the effect of pin on disc wear test on wear rate is analyzed.

## 2. Materials and Methods

Inconel 625 is selected as the substrate owing to its usage in aerospace industries and heat exchangers manufacturers. Electroless coating technique is chosen to coat on the substrate to improve the wear resistivity. The following steps are about the preparation of the electroless solution:

- (i) Take the required vessels, rinse it with soap water, and clean it with deionized water.
- (ii) Take 200 ml of nickel phosphorous solution in 250 ml beaker and place it in a magnetic stirrer until it obtains temperature of 88°C which is measured by thermometer.
- (iii) Take a sample of Inconel 625, rinse it with soap water, and clean it with deionized water. Now, clean the sample using ultrasonic cleaner at 55°C.
- (iv) Take the cleaned sample and dip it in a solution containing 50% of HCl. Now, prepare the MWCNT solution by adding sodium lauryl sulphate in deionized water.
- (v) Place the sample in the holder which is dipped inside the Nickel phosphorous solution; after half an hour, add 0.30 g of MWCNT and leave the sample for 1 hour.
- (vi) Now, take the sample, again clean it with deionized water, and dry it.
- (vii) Place the sample in the holder which is dipped inside the Nickel phosphorous solution, and leave the sample for 1 ½ hours in the magnetic stirrer.

The specimens are machined equal to 20 mm and cleaned using acetone and diluted HCL, and the specimens are dried. Figure 1 shows the wear test assembly and specimen. The sample size ranges with 20 mm diameters and 15 mm length. The specifications of Pin on disc are as follows: Load (N):5–200 N; disc speed: 100–2000 rpm; motor and drive: AC motor with drive; sliding velocity: 0.5 to 10 m/s; specimen holders: universal holders; wear measurement ( $\mu$ ):  $\pm 5000$  microns or  $\pm 5$  mm.

### 3. Taguchi Analysis

Taguchi analysis is used to design the experiment and it gives reduced variance for the experiment with optimum settings of process factors. The orthogonal array would provide a complete set of very well balanced design of experiments. Taguchi analysis consist experiments' plan, model determination, and adequacy check of the predictive model. Furthermore, it comprises of planning of experiments, determination of model, and checking adequacy of the developed model. The parameters selected to study the wear behavior of the coated work material are sliding distance, velocity, and load. Experiment's plan is carried out by Taguchi analysis. The  $L_{27}$  experimental trails are done for the chosen number of factors. Table 1 shows the factors and their levels. Figure 2 shows the SEM images of the coated

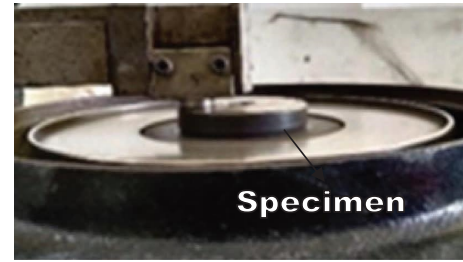


FIGURE 1: Wear test tribometer.

specimen, in which the CNTs (Carbon Nano Tubes) are agglomerated on the substrate.

### 4. Wear Test

The sliding wear behaviour is studied on the coated Inconel 625 specimen to observe the impact of MWCNT on the improvement of wear resistance. Load applied on the specimen and the specimen adheres to the counterface. The specimen is kept close to this counter face. The disc is cleaned and polished using SiC emery sheets to have clean surface contact of coated specimen surface. The parameters are set in the pin on disc setup, and tests are carried out based on  $L_{27}$  orthogonal array. The rate of wear is evaluated by weight loss way as shown in equation (1). The weight of the specimen is calculated before and after the wear test.

$$W = \frac{M}{\rho} * D, \quad (1)$$

where  $W$  = wear rate (WR) ( $\text{mm}^3/\text{m}$ ),  $M$  = weight loss (WL) (g),  $\rho$  = density ( $\text{g}/\text{mm}^3$ ),  $D$  = sliding distance (SL) (m).

### 5. Results and Discussions

The impact of wear factors on the MWCNT-coated Inconel 625 substrate is analyzed with the help of ANOVA analysis.

The wear test based on 27 experimental trails was carried out and Table 2 shows wear test results. The experimental results are analyzed through the Design Expert, and a predictive model is developed to predict the rate of wear. Table 3 shows the estimation of the coefficients for the development of a model and significance test of the model. The wear rate is expressed in equation (2) using the regression coefficient as given in Table 3, and the average percentage error is found to be within 0.99%. Table 4 shows the difference among the experimental results and forecasted results. The other new levels of factors are substituted in the developed model and verified the model results with experimental results. The comparison of actual with predicted results is shown in Figure 3.

$$\begin{aligned} \text{Wear rate} = & 0.000749 + 0.000014 * \text{load} + 0.000033 * \text{Velocity} + 3.72778E - 08 * \text{Sliding distance} - 6.52778E \\ & - 07 * \text{load} * \text{velocity} - 2.88333E - 09 * \text{load} * \text{sliding distance} - 3.67778E - 08 * \text{Velocity} * \text{sliding distance}. \end{aligned} \quad (2)$$

TABLE 1: Factors/levels.

S. no	Factors	Levels
1	Load ( $L$ ) (N)	10 30 50
2	Velocity ( $V$ ) (m/s)	1.5 3 4.5
3	Sliding distance (SL) (m)	500 1000 1500

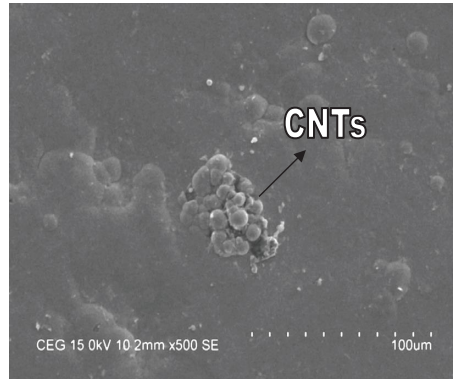


FIGURE 2: SEM images of MWCNT coated specimen.

TABLE 2: Experimental results of wear rate: coated inconel 625.

Exp	Load (N)	Velocity (m/s)	Sliding distance (m)	Wear rate ( $\text{mm}^3/\text{m}$ )
1	10	1.5	500	0.000930
2	10	1.5	1000	0.000905
3	10	1.5	1500	0.000877
4	10	3	500	0.000921
5	10	3	1000	0.000856
6	10	3	1500	0.000707
7	10	4.5	500	0.000912
8	10	4.5	1000	0.000838
9	10	4.5	1500	0.00095
10	30	1.5	500	0.001144
11	30	1.5	1000	0.001107
12	30	1.5	1500	0.001068
13	30	3	500	0.001156
14	30	3	1000	0.001064
15	30	3	1500	0.000911
16	30	4.5	500	0.001114
17	30	4.5	1000	0.001041
18	30	4.5	1500	0.000803
19	50	1.5	500	0.001338
20	50	1.5	1000	0.001312
21	50	1.5	1500	0.001271
22	50	3	500	0.001362
23	50	3	1000	0.001231
24	50	3	1500	0.001108
25	50	4.5	500	0.001351
26	50	4.5	1000	0.001226
27	50	4.5	1500	0.001097

**5.1. Analysis of Variance.** The factor's significance on the wear rate is estimated with the help of ANOVA (Analysis of Variance) analysis. Table 5 shows ANOVA analysis.  $R^2$  and adjusted  $R^2$  such as 91% and 89%, respectively, for significance test are evident that the model developed correlate very well the factors with the wear rate. The ANOVA is used

to estimate the impact of every factor. The  $P$ -value indicates the statistical importance of every factor. The particular factor can be said to be statically important, if the  $P$ -value is identified to be lesser than 0.05. The ANOVA is set with the significance level of 5%. The  $F$ -value for every factor on wear rate is evaluated as Load (175.62), velocity (5.84) and sliding

TABLE 3: Significant test results: wear rate.

Term	Coeff	SE coeff	T	P
Constant	0.0011	6.136E-06	0.0010	0.0011
Load	0.0002	7.516E-06	0.0002	0.0002
Velocity	-0.0000	7.516E-06	-0.0001	-0.0001
Sliding distance	-0.0001	7.516E-06	-0.0001	-0.0001
Load*velocity	1.750E-06	9.205E-06	-0.0000	0.0001
Load*sliding distance	-7.250E-06	9.205E-06	-0.0000	0.0001
Velocity*sliding distance	-0.0000	9.205E-06	-0.0001	-0.0001

TABLE 4: Predicted vs. experimental trial values.

S. no	Actual	Predicted	Percentage error (%)
1	0.0009	0.0009	0.00
2	0.0009	0.0009	0.00
3	0.0009	0.0009	0.00
4	0.0009	0.0009	0.00
5	0.0009	0.0008	12.50
6	0.0007	0.0008	12.50
7	0.0009	0.0009	0.00
8	0.0008	0.0008	0.00
9	0.0007	0.0007	0.00
10	0.0011	0.0011	0.00
11	0.0011	0.0011	0.00
12	0.0011	0.0011	0.00
13	0.0012	0.0011	9.09
14	0.0011	0.0011	0.00
15	0.0009	0.0010	10.00
16	0.0011	0.0011	0.00
17	0.0010	0.0010	0.00
18	0.0008	0.0009	11.11
19	0.0013	0.0014	7.14
20	0.0013	0.0013	0.00
21	0.0013	0.0012	8.33
22	0.0014	0.0014	0.00
23	0.0012	0.0013	7.69
24	0.0011	0.0012	8.33
25	0.0014	0.0014	0.00
26	0.0012	0.0012	0.00
27	0.0011	0.0011	0.00

distance (31.33). The *F*-value of every factor on wear rate, the load, and sliding distance is identified to be a more significant impact on wear rate followed by velocity as shown in Table 5.

5.2. *Influence of Factors on Wear Rate.* The 3D plot developed to study the wear rate as the level of the wear test factors such as load, and sliding distance is shown in Figures 4(a)–4(c). The changes in wear rate at the various level of load and velocity is shown in Figure 4(a). From this Figure 4(a), it is seen that the wear has increased with increase in the level of load and it would be owing to generation of higher pressure and higher stresses during the measurement. However, MWCNT coating on the substrate minimizes the deformation owing to good

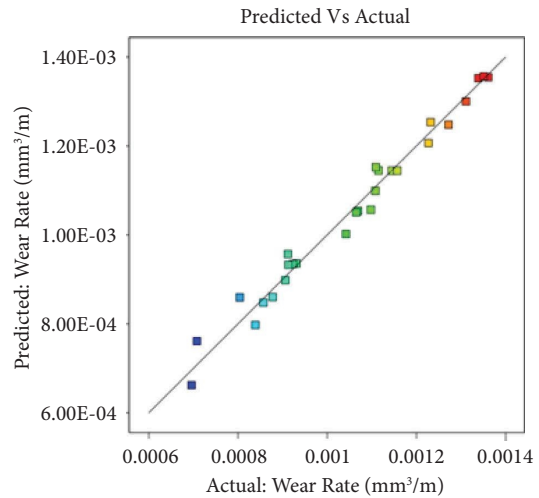


FIGURE 3: Predicted vs. experimental results.

TABLE 5: ANOVA results for wear rate.

Source	SoS	DF	MS	F	P
Model	8.018E-07	6	1.336E-07	36.54	<0.0001
Load	6.422E-07	1	6.422E-07	175.62	<0.0001
Velocity	2.136E-08	1	2.136E-08	5.84	0.0253
Sliding distance	1.146E-07	1	1.146E-07	31.33	<0.0001
Load*velocity	4.602E-09	1	4.602E-09	1.26	0.2752
load*sliding distance	9.976E-09	1	9.976E-09	2.73	0.1142
velocity*sliding distance	9.130E-09	1	9.130E-09	2.50	0.1298
Residual	7.314E-08	20	3.657E-09		
Total	8.750E-07	26			

$R^2$ : 91% and adjusted:  $R^2$  89%.

adherability, stability, and adequate wear resistivity. Lower wear is seen at 10 N load due to lower pressure via lever arm (tribometer/pin on disc). The wear rate increases as the velocity level is reduced, and it would be owing to high contact/interaction time among the disc and the specimen. The change in the wear rate due to change in the level of sliding distance is shown in Figures 4(a) and 4(b). The wear rate is found to be high at lower level of sliding distance and the wear rate is reduced as the level of sliding distance is increased. At low sliding distance, the wear rate is increased. It would owe some irregularities presented in the coating process, and these irregularities would induce improper contact of disc with specimen surface. The worn out surfaces of the coated Inconel 625 are examined with help of SEM as shown in Figure 5. The coated Inconel surfaces worn out at various levels of pin on disc factors are examined. The worn pot coated surface at various levels of the tribometer’s factors is shown in Figures 5(a) and 5(b). The minimum of scratches with merciful wear is seen at lower level of load, middle and higher level of velocity, and higher level of sliding distance as shown in Figures 5(a) and 5(b), and it would be owing to minimum pressure induced on the pin on disc.

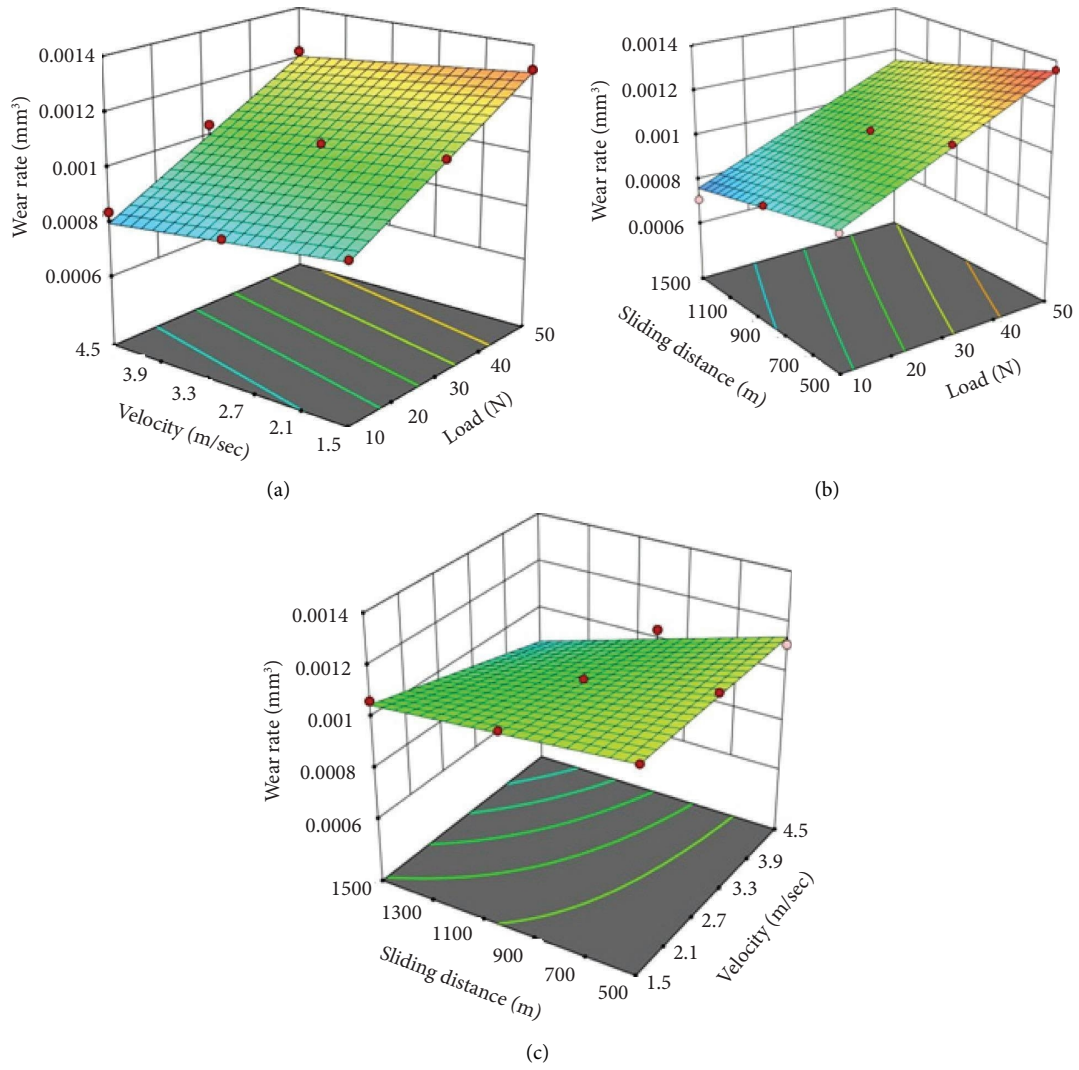


FIGURE 4: Wear rate at various levels of factors. (a) Wear rate: V vs. L; (b) Wear rate: SD vs. L; (c) Wear rate: SD vs. V.

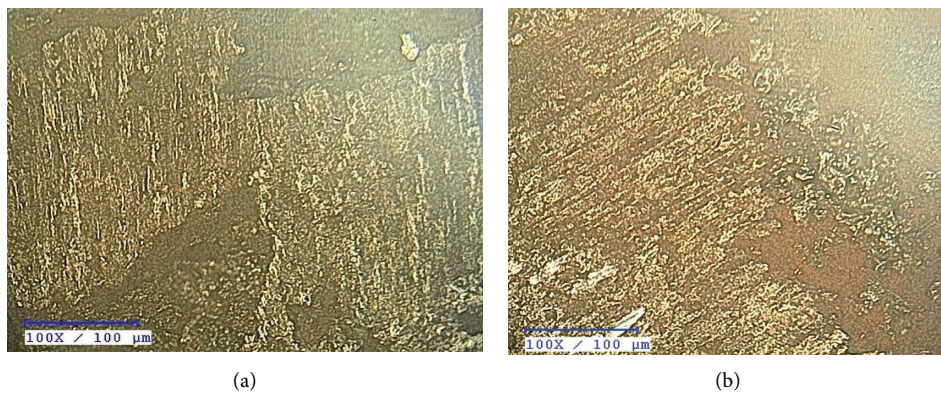


FIGURE 5: (a-b) Worn out images of the coated surface. (a) Worn out images at 10 N, 4.5 m/sec and 1000 m. (b) Worn out image at 10 N, 3 m/sec and 1500 m.

## 6. Conclusion

MWCNT is deposited on the Inconel 625 through the Ni-P electroless coating method. The following conclusions were observed:

- (i) A predictive model is developed to predict the wear rate and it facilitates a best relation among pin on disc wear process factors with wear rate of MWCNT coated specimen.
- (ii) ANOVA test provides and confirms the adequacy of the model with very minimum lack of fit.
- (iii) Load is influenced significantly on wear rate followed by sliding distance and velocity.
- (iv) The plot of wear rate at various levels of wear process factors shows that increase in load develops the wear rate. The increase in velocity and sliding distance diminishes the rate of wear.
- (v) The maximum wear rate observed at load = 50 (N),  $V = 3$  (m/sec),  $SD = 500$  (m) is found to be 1.92 times higher than the wear rate observed at load = 10 (N),  $V = 3$  (m/sec),  $SD = 1500$  (m).
- (vi) The presence of coating has been ensured via scanning electron microscopy analysis.

## Data Availability

The data used to support the findings of this study are included within the article.

## Conflicts of Interest

The authors declare that they have no conflicts of interest.

## References

- [1] P. Sivaprakasam, P. Hariharan, and G. Elias, "Experimental investigations on magnetic field-assisted micro-electric discharge machining of inconel alloy," *International Journal of Ambient Energy*, vol. 43, no. 1, pp. 2619–2626, 2022.
- [2] P. Sivaprakasam and P. Hariharan, "Optimization of process parameters of micro-WEDM process on inconel super alloy through response surface methodology," *International Journal of Mechanical and Production Engineering Research and Development*, vol. 8, no. 6, pp. 1001–1012, 2018.
- [3] Q. Naji, J. M. Salman, and N. M. Dawood, "Investigations of structure and properties of layered bioceramic HA/TiO<sub>2</sub> and ZrO<sub>2</sub>/TiO<sub>2</sub> coatings on Ti-6Al-7Nb alloy by micro-arc oxidation," *Materials Today Proceedings*, vol. 61, 2021.
- [4] Y. Guo, L. Xu, J. Luan, Y. Wan, and R. Li, "Effect of carbon nanotubes additive on tribocorrosion performance of micro-arc oxidized coatings on Ti6Al4V alloy," *Surfaces and Interfaces*, vol. 28, pp. 101626–101713, 2022.
- [5] Z. Li, Z. Cai, X. J. Cui, R. Liu, Z. Yang, and M. Zhu, "Influence of nanoparticle additions on structure and fretting corrosion behavior of micro-arc oxidation coatings on zirconium alloy," *Surface and Coatings Technology*, vol. 410, no. 25, Article ID 126949, 2021.
- [6] R. Askarnia, S. R. Fardi, M. Sobhani, H. Staji, and H. Aghamohammadi, "Effect of graphene oxide on properties of AZ91 magnesium alloys coating developed by micro-arc oxidation process," *Journal of Alloys and Compounds*, vol. 892, no. 5, Article ID 162106, 2022.
- [7] R. Küçükosman, E. Emine Şüküroğlu, Y. Totik, and S. Şüküroğlu, "Investigation of wear behavior of graphite additive composite coatings deposited by micro arc oxidation-hydrothermal treatment on AZ91 Mg alloy," *Surfaces and Interfaces*, vol. 22, Article ID 100894, 2021.
- [8] V. C. Thanu, C. Andrew, and M. Jayakumar, "Electrodeposition of nickel super alloy from deep eutectic solvent," *Surfaces and Interfaces*, vol. 19, Article ID 100539, 2020.
- [9] T. M. Reis, C. D. Boeira, F. L. Serafini, M. C. M. Farias, C. A. Figueroa, and A. F. Michels, "Micro-abrasive wear resistance of heat-treated electroless nickel phosphorus coatings deposited on copper beryllium alloy C17200," *Surface and Coatings Technology*, vol. 438, Article ID 128374, 2022.
- [10] J. Corona-Gomez, K. K. Sandhi, and Q. Yang, "Wear and corrosion behaviour of nano crystalline TaN, ZrN, and TaZrN coatings deposited on biomedical grade CoCrMo alloy," *Journal of the Mechanical Behavior of Biomedical Materials*, vol. 130, 2022.
- [11] B. Wei, Y. Cheng, Y. Liu, Z. Zhu, and Y. Cheng, "Corrosion and wear resistance of AZ31 Mg alloy treated by duplex process of magnetron sputtering and plasma electrolytic oxidation," *Transactions of Nonferrous Metals Society of China*, vol. 31, no. 8, pp. 2287–2306, 2021.
- [12] X. Ma, S. Jin, R. Wu et al., "Influence alloying elements of Al and Y in MgLi alloy on the corrosion behavior and wear resistance of microarc oxidation coatings," *Surface and Coatings Technology*, vol. 432, Article ID 128042, 2022.
- [13] C. Jiang, J. Zhang, Y. Chen et al., "On enhancing wear resistance of titanium alloys by laser clad WC-Co composite coatings," *International Journal of Refractory Metals and Hard Materials*, vol. 107, Article ID 105902, 2022.
- [14] B. Qin, S. Zhou, H. Chen, and M. Wang, "Superior corrosion and wear resistance of AZ91D Mg alloy via electrodeposited SiO<sub>2</sub>-Ni-based composite coating," *Materials Chemistry and Physics*, vol. 283, Article ID 126001, 2022.
- [15] A. Divya Sadhana, J. Udaya Prakash, P. Sivaprakasam, and S. Ananth, "Wear behaviour of aluminium matrix composites (LM25/Fly ash)-A Taguchi approach," *Materials Today: Proceedings*, vol. 33, pp. 3093–3096, 2020.
- [16] P. Sivaprakasam, A. Kirubel, G. Elias, P. Maheandera Prabu, and P. Balasubramani, "Mathematical modeling and analysis of wear behavior of AlTiN coating on titanium alloy (Ti-6Al-4V)," *Advances in Materials Science and Engineering*, vol. 2021, Article ID 1098605, 9 pages, 2021.
- [17] P. Sivaprakasam, G. Elias, P. Maheandera Prabu, and P. Balasubramani, "Experimental investigations on wear properties of AlTiN coated 316LVM stainless steel," *Materials Today: Proceedings*, vol. 33, pp. 3470–3474, 2020.
- [18] M. K. Hassanzadeh-Aghdam, M. J. Mahmoodi, and J. Jamali, "Effect of CNT coating on the overall thermal conductivity of unidirectional polymer hybrid nanocomposites," *International Journal of Heat and Mass Transfer*, vol. 124, pp. 190–200, 2018.
- [19] C. Yang, S. Song, F. Chen, and N. Chen, "Fabrication of PVDF/BaTiO<sub>3</sub>/CNT piezoelectric energy harvesters with

- bionic balsa wood structures through 3D printing and supercritical carbon dioxide foaming,” *ACS Applied Materials & Interfaces*, vol. 13, no. 35, pp. 41723–41734, 2021.
- [20] Z. Ye, J. Li, L. Liu, F. Ma, B. Zhao, and X. Wang, “Microstructure and wear performance enhancement of carbon nanotubes reinforced composite coatings fabricated by laser cladding on titanium alloy,” *Optics & Laser Technology*, vol. 139, Article ID 106957, 2021.
- [21] N. Radhika and R. Raghu, “Influence of parameters on sliding wear of titanium nitride coated 6061 aluminium alloy,” *Tribology in Industry*, vol. 40, no. 2, pp. 203–212, 2018.